Fractional Calculus & Applied Analysis
An International Journal for Theory and Applications
VOLUME 21, NUMBER 3 (2018)
(Print) ISSN 1311-0454
(Electronic) ISSN 1314-2224

RESEARCH PAPER

NOVEL POLARIZATION INDEX EVALUATION FORMULA AND FRACTIONAL-ORDER DYNAMICS IN ELECTRIC MOTOR INSULATION RESISTANCE

Emmanuel A. Gonzalez [1], Ivo Petráš [2], Manuel D. Ortigueira [3]

Abstract

One of the common test metrics prescribed by IEEE Std 43 for testing motor insulation is the Polarization Index (P.I.) which evaluates the "goodness" of the machine's insulation resistance by getting the ratio of the insulation resistance measured upon reaching $t_2 > 0$ minutes (IR_{t2}) from $t_1 > 0$ minutes (IR_{t2}) for $t_2 > t_1 > 0$, after applying a DC step voltage. However, such definition varies from different manufacturers and operators despite of decades of research in this area because the values of t_1 and t_2 remain to be uncertain. It is hypothesized in this paper that the main cause of having various P.I. definitions in literature is due to the lack of understanding of the electric motor's dynamics at a systems level which is usually assumed to follow the dynamics of the exponential function. As a result, we introduce in this paper the fractional dynamics of an electric motor insulation resistance that could be represented by fractional-order model and where the resistance follows the property of a Mittag-Leffler function rather than an exponential function as observed on the tests done on a 415-V permanent magnet synchronous motor (PMSM). As a result, a new PMSM health measure called the Three-Point Polarization Index (3PPI) is proposed.

MSC 2010: Primary 26A33; Secondary 94C12, 47E05

pp. 613–627 , DOI: 10.1515/fca-2018-0033
DE GRUYTER

Key Words and Phrases: electric motors, fractional calculus, insulation testing, permanent magnet motors, transfer functions, Mittag-Leffler function

1. **Introduction**

The aging of the mechanical, electrical and chemical properties of electric motors is a very important consideration in determining its overall health condition to avoid unwanted breakdowns and potential unsafe and hazardous operations [14, 20, 21, 28, 8]. In fact, a low resistance value of the electric motor could cause catastrophic failures in the electronic driver circuit that supplies power to the machine. Damage in its thyristors, for example, could cause heavy financial losses due to thyristor replacement and circuit board repair—a well-known consequence of high repair cost in industries using electric machines in general [4], for example, in an elevator industry employing condition-based approaches in equipment maintenance [9]. In practice, the most common measure being used in determining the motor's health is through the measurement of insulation resistance which, based on fundamental physics, is proportional to the type and geometry of insulation used, and is inversly-proportional to the conductor surface area.

There are many ways in determining the health of an electric motor through its insulation resistance which are all discussed in the IEEE Recommended Practice for Testing Insulation Resistance of Electric Machinery, IEEE Std 43-2013 [16]. One simple test that is employed is the Polarization Index (P.I.) test which is normally defined in this standard as the ratio of the insulation resistance measured upon reaching 10 minutes, i.e. IR_{10}, with respect to the insulation resistance measured upon reaching 1 minute, i.e. IR_1, which can be described mathematically as

$$P.I. = \frac{IR_{10}}{IR_1}, \tag{1.1}$$

from an input step voltage that is appropriate for the winding voltage ratings. The IEEE Std 43-2013 recommends the following insulation resistance test DC step voltages which is presented in Table 1 for convenience. In some cases the time values of the insulation resistance measurement varies depending on the specifications of the motor which is then prescribed by the original equipment manufacturer (OEM), or based on the evaluation of the experienced electric motor operators from the applied condition-based and preventive maintenance programs. This is true especially for form-wound stators employing modern insulation systems where tests could be done between 1 to 5 minutes only. Such observation is also valid for generator stator insulations [19, 25].

Winding rated voltage	Insulation resistance test DC voltage
< 1000 V	500 V
1000 to 2500 V	500 to 1000 V
2501 to 5000 V	1000 to 2500 V
5001 to 12000 V	2500 to 5000 V
> 12000 V	5000 to 10000 V

Table 1. Insulation resistance test DC voltages based on electric motor winding rated voltage.

According to IEEE Std 43, to evaluate the health of an electric machine, one must ensure the recommended minimum values of polarization index depending on the thermal class ratings of the insulation used are avoided. These values are presented in Table 1. For modern electric motors, if the insulation resistance at 1 minute goes beyond 5000 MΩ, then the use of the P.I. test may result in a wrong evaluation if used further since the measured total current is already too small for proper analysis. In this range, sensitivity issues from the test equipment itself on supply voltage, humidity conditions and test setup could already compromise the readings that is why the P.I. is not anymore recommended [16].

Thermal class rating	Minimum P.I.
Class 105 (A)	1.5
Class 130 (B) and above	2.0

Table 2. Recommended minimum values of polarization index for different types of insulation thermal class ratings.

One of the issues faced in using the P.I. as a test parameter is that there is still no standard in determining the time intervals in the P.I. test. Unfortunately, different organizations and OEMs would have their own definitions. This then makes the minimum recommended P.I. values in Table 1 somewhat unreliable in a sense. Furthermore, until now, there is no pass-fail criteria which can be used from the P.I. value observed. As a matter of practice, one could simply compute for the P.I. of the machine, then makes an evaluation based on years of experience in determining if a repair job, e.g. motor reconditioning or rewinding, needs to be done. In effect, the standard in [16], when it comes to the P.I., could result in an uncertainty where the operator has the opportunity to make his own decisions beyond what is recommended by the standard.

We assumed in this paper that one of the reasons on why the P.I. definition is not well-established is because there is no direct way of establishing an appropriate relationship between the time duration for the P.I. test based on the dynamics of electric motor. The dynamics of the electric machine is not well-understood from the systems theory point-of-view, despite of heavy research in the analysis of the total current measured in an electric motor with respect to the motor's absorption current, conduction current, geometric capacitive current and surface leakage current—all well-explained in [16, 2, 3]. However, one can simply assume that the relationship of the output computed insulation resistance with respect to a step input dc voltage would follow a simple first-order or overdamped second-order system of the forms:

$$G_1\left(s\right)=\frac{Y\left(s\right)}{E\left(s\right)}=\frac{K}{Ts+1}, \tag{1.2}$$

for $K, T > 0$ and

$$\begin{aligned} G_2\left(s\right)&=\frac{Y\left(s\right)}{E\left(s\right)}=\frac{K\omega_n^2}{s^2+2\zeta\omega_n s+\omega_n^2},\\ &=\frac{K}{\left(T_1 s+1\right)\left(T_2 s+1\right)} \end{aligned} \tag{1.3}$$

for $K, T_1, T_2, \omega_n > 0$ and $\zeta > 1$, respectively. If the dynamics of the electric motor is assumed to follow the models in (1.2) and (1.3), then the insulation resistance values with respect to time should follow the dynamics of the usual exponential function in the form of

$$y\left(t\right)=K\left(1-e^{-t/T}\right),\quad t\geq 0, \tag{1.4}$$

for the first order system in (1.2), and

$$y\left(t\right)=K\left(1-\frac{T_1}{T_2-T_1}e^{-t/T_2}-\frac{T_2}{T_2-T_1}e^{-t/T_1}\right),\quad t\geq 0, \tag{1.5}$$

for the overdamped second-order system in (1.3). However, upon experimentation on a low-power 415-V permanent magnet synchronous motor (PMSM) used in a high-rise elevator, it was discovered that the insulation resistance dynamics do not follow (1.4) nor (1.5). In fact, upon using fractional calculus [24, 27], it was assumed that the model should appropriately follow the fractional-order transfer function (FOTF)

$$G_F\left(s\right)=\frac{K}{Ts^{\alpha}+1}, \tag{1.6}$$

for $K, T > 0$ and where $0 < \alpha < 1$ is the order of the model.

The above transfer function (1.6) corresponds to a simple fractional-order differential equation (FODE) of the form

$$T\frac{d^{\alpha}}{dt^{\alpha}}y_F\left(t\right)+y_F\left(t\right)=Ku\left(t\right), \tag{1.7}$$

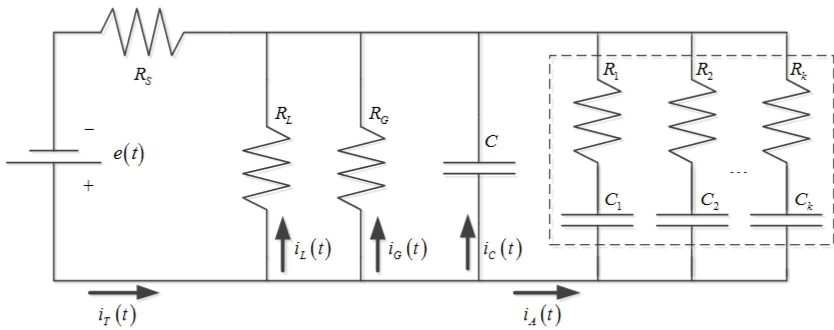

FIGURE 1. Equivalent circuit of an electric motor as shown in Fig. 1 of IEEE Std 43-2013, [16].

where $y_F(t)$ being an output function and $u(t)$ being the unit-step function.

The solution of the FODE (1.7) for $0 < \alpha < 1$ is [23]

$$y_F(t) = \frac{K}{T} t^{\alpha} \sum_{k=0}^{\infty} \frac{\left[\left(-\frac{1}{T}\right) t^{\alpha}\right]^k}{\Gamma(\alpha k + \alpha + 1)} = \frac{K}{T} t^{\alpha} E_{\alpha,\alpha+1}\left(-\frac{t^{\alpha}}{T}\right), \tag{1.8}$$

where $E_{\mu,\beta}(z)$ is two-parameters Mittag-Leffler function [7].

The general theory of insulation resistance and reason why a fractional-order system is suitable in modeling a PMSM is described in Section 2. The development of a fractional-order model for a low-power PMSM is discussed in Section 3, while discussion on its effects in polarization index is presented in Section 4. A new insulation resistance measure called the Three-Point Polarization Index (3PPI) is also presented in Section 4. Section 5 concludes this paper with some additional remarks for further research.

This paper serves as an extended version of a previous conference paper [10].

2. General theory of insulation resistance

The equivalent circuit of an electric motor is shown in Fig. 1, emphasizing on the current flowing into its branches. The total current, $i_T(t)$, is a function of the following currents: the surface leakage current, $i_L(t)$, the conduction current, $i_G(t)$, the geometric capacitive current, $i_C(t)$, and the absorption current, $i_A(t)$. $e(t)$ is the supplied voltage into the electric motor while $R_S, R_L, R_G, R_1, R_2, \cdots, R_k, C, C_1, C_2, \cdots, C_k$ for $k \in \mathbb{Z}^+$ are resistors and capacitors representing the overall characteristics of the electric motor.

From Fig. 1, it can be seen that the absorption current, $i_A(t)$, is defined by an RC ladder where the values of its resistances and capacitances depend on the properties, type, and most importantly the condition of the insulation system. In all of the currents flowing into the machine, the absorption current, $i_A(t)$, is considered to be the one that has the biggest impact in defining how the insulation resistance would change with respect to time. In IEEE Std 43-2013 [16], the absorption current, $i_A(t)$, is normally expressed as an inverse power function of time. The absorption current, $i_A(t)$, results from electron drift and molecular polarization of the insulation [5, 26, 15, 33].

However, such similar phenomenon has been existing in many other systems such as electrode/electrolyte-based systems including the Warburg impedance and other similar interfaces [32, 30, 18], and those systems with electrodes connected in porous channels [17], where the total impedance follows a power law that is fractional degree in value. The realization of such fractional-power-law impedances was generally described by Wang [31] as a resistor-capacitor (RC) ladder network which can be mathematically expressed using continued fraction expansions which would end up in a circuit having a constant phase throughout the frequency spectrum, or basically a fractional-order element with a fractional-order impedance of the form

$$Z(j\omega) = (j\omega)^{\alpha}, \tag{2.1}$$

where $0 < \alpha < 1$. Practically, since the entire frequency spectrum cannot be satisfied, approximation models by Valsa [29] were used where the RC ladder network is truncated at a certain extent, making the circuit valid for a certain limited range of frequencies [13]. Approaches in the implementation of such circuits where then attempted throughout the years for industrial controllers [6, 12], design of signal processing filters [22], and microelectronic circuits [1].

Combining all the resistances and capacitances in Fig. 1, except for R_S, would result in a similar case of an RC ladder with a fractional-order impedance. In such case, the total admittance of the RC ladder with respect to the resistors and capacitors in Fig. 1 becomes

$$Y(j\omega) = \frac{1}{R_L||R_G} + j\omega C + \sum_{k=1}^{m} \frac{j\omega C_k}{1 + j\omega R_k C_k}, \tag{2.2}$$

where

$$\omega = [\omega_{\min}, \omega_{\max}] \,\widetilde{\in}\, \left[\frac{1}{R_1 C_1}, \frac{R_1 C_1}{\left(\frac{0.24}{1+\triangle\varphi}\right)^{m}}\right] \tag{2.3}$$

is the range of frequencies in rad/s, $m > 0$ is the number of RC branches in the ladder network, and $\triangle\varphi > 0$ is a certain small value of phase ripple in degrees which is allowed to satisfy the approximation in the constant phase region from $\omega_{\min}$ to ω_{max}. The symbol $\widetilde{\in}$ indicates that the lower and upper limits of the frequency range are just approximate values, i.e. $\omega_{\min} \approx$

$1/R_1C_1$ and $\omega_{max} \approx R_1C_1\left(0.24/1+\triangle\varphi\right)^{-m}$. The readers are referred to [13] for the derivation of (2.2) and (2.3). Combining R_S and the fractional-order element from the combination of R_L, R_G, R_1, $R_2, \cdots, R_k$, C, C_1, $C_2, \cdots, C_k$, which is described by the admittance in (2.2) would then result in a resistor-fractional-order-element series circuit with a total impedance of

$$Z\left(s\right) = R_S + Ms^{\alpha},$$

where $M > 0$ is a certain resistive magnitude. Discussion on the properties of such circuit are presented in [11]. This then justifies the mathematical basis for assuming that a PMSM could be represented by a fractional-order dynamical model as discussed in the next section.

3. **Development of a fractional-order dynamical model for a PMSM**

Time [mins.]	L1-L2 Res. [MΩ]	L2-L3 Res. [MΩ]	L3-L1 Res. [MΩ]
0	61	67	67
1	193	213	216
2	232	249	252
3	248	264	267
4	258	271	273
5	266	276	277
6	270	278	278
7	275	280	279
8	286	281	281
9	283	283	281
10	284	289	281

TABLE 3. Insulation resistance values gathered on a 415-V PMSM used in a high-risk elevator system between two different lines.

Throughout this section, we focus on the resistance data obtained in L3-L1. Without using any sophisticated system identification algorithm and from a simple trial-and-error routine, the FOTF model identified results in

$$G_{F,L3-L1}\left(s\right) = \frac{0.57}{15s^{0.81}+1}, \tag{3.1}$$

where the order of the system becomes $\alpha = 0.81$. The step response of (3.1) from 500-Vdc step input is shown in Fig. 3 together with the data in Table 3 for L3-L1. In Fig. 3 a plot of (3.1) is discretized every 60 seconds for compatibility with the data obtained through the Fluke 1503 insulation resistance tester.

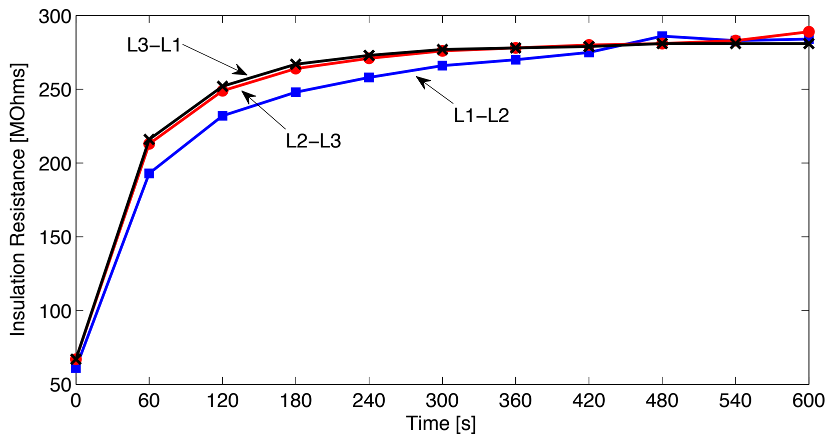

FIGURE 2. Insulation resistance measured on different time values from 0 to 10 mins from an input DC step voltage of 500 Vdc. Blue line with square markers are for L1-L2. Red line with circular markers are for L2-L3. Black line with cross markers are for L3-L1.

PMSM Specifications	**Data**
Insulation class	F (Thermal class 130)
Moment of intertia [kg·m^2]	4.0
Rated voltae [V]	380 to 480 $\pm$10%
Rated current [A]	0.65
Degree of protection	IP 21

TABLE 4. Specifications of the PMSM tested for insulation resistance.

The data gathered from a 415-V PMSM through a Fluke 1503 insulation resistance tester are shown in Table 3. Plots of the data are also presented in Fig. 2. The specifications of the motor tested are shown in Table 4.

Using (1.8), the step response of (3.1) from a 500-Vdc step input yields

$$\begin{aligned} y_F(t) &= 500\left(\frac{0.57}{15}\right)t^{0.81}\sum_{k=0}^{\infty}\frac{\left[\left(-\frac{1}{15}\right)t^{0.81}\right]^k}{\Gamma(0.81k+0.81+1)} \\ &= 19t^{0.81}\sum_{k=0}^{\infty}\frac{\left[-0.0667t^{0.81}\right]^k}{\Gamma(0.81k+1.81)} \\ &= 19t^{0.81}E_{0.81,1.81}(-0.0667t^{0.81}), \end{aligned} \tag{3.2}$$

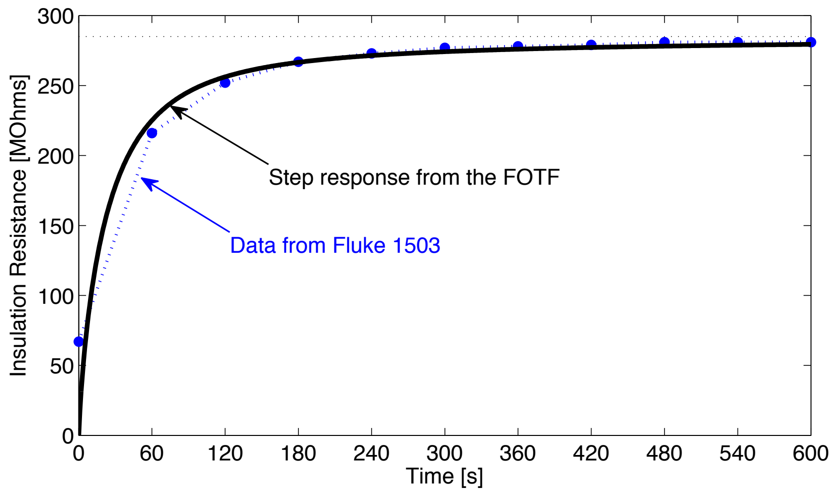

FIGURE 3. 500-V step response of the FOTF in (3.1) with respect to the data plot from Table 3 for L3-L1. Dashed-blue line with circular markers represents Table 3 L3-L1 data plot while the solid-black line represents the step response in (3.1). Unit-step response is from a 500-Vdc step input.

by letting $K = 0.57$, $T = 15$ secs., $\alpha = 0.81$, and by scaling the entire function with 500 units to incorporate the effect of the 500-Vdc step input voltage. It can be concluded from the point of view of L3-L1, the motor insulation resistance is a 0.81-order system.

4. Characteristics of the fractional-order dynamics in relation to polarization index

The P.I. method is known as a good indicator in determining if the insulation of the PMSM is already at fault. However, the type of fault may not necessarily be identified from the value itself. In fact, the severity of the fault could cause various result in the P.I. value. Although it is understood that the P.I. alone may not be able to provide a detailed picture of the condition of the motor, it is still a parameter that has to be identified in relation to the dynamics of the PMSM's insulation resistance over time due to practical reasons.

The P.I. formula in (1.1) itself could be misleading because it only measures the 1st and 10th minute insulation resistance values without regards to the dynamics. To illustrate this situation, consider the approximate FOTF in (3.1) and another hypothetical FOTF

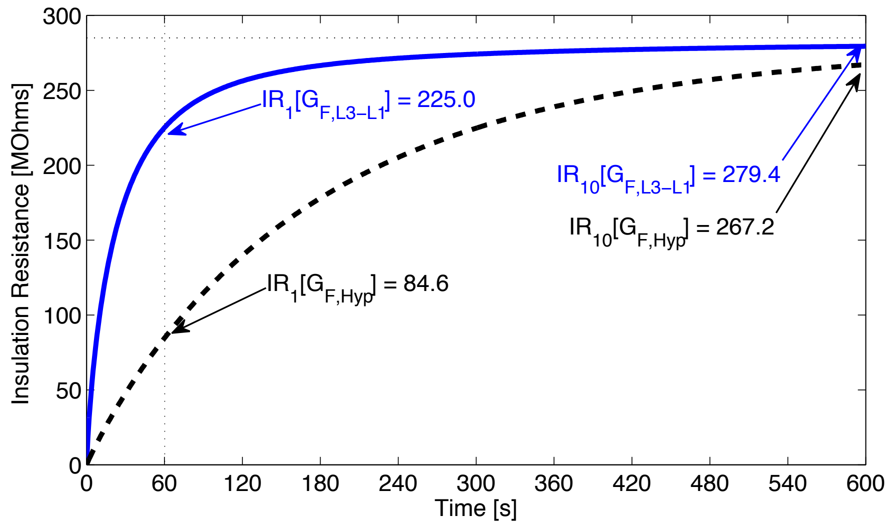

FIGURE 4. 500-V step responses of (3.1) and (4.1). The solid-blue line represents $G_{F,L3-L1}$ while the dashed-black line represents $G_{F,Hyp}$.

$$G_{F,Hyp}(s) = \frac{0.57}{140s^{0.95}+1}, \tag{4.1}$$

both of its step responses with a 500-Vdc step input voltage shown in Fig. 4. At a first glance, one can see that the two responses are different in shape: $G_{F,L3-L1}(s)$ looks "healthier" than $G_{F.Hyp}(s)$ because the insulation resistance of $G_{F,L3-L1}(s)$ has reached a stabilizing point upon reaching around 120 seconds. On the other hand, the step response of $G_{F,Hyp}(s)$ has significant and highly-sloped monotonically growth throughout the 10-minute period. The graphical evaluation is counterintuitive when compared to their respective P.I. values. For $G_{F,L3-L1}(s)$, the measured P.I. value is

$$P.I.[G_{F,L3-L1}] \approx \frac{279.4}{225.0} \approx 1.2, \tag{4.2}$$

while the P.I. value measured for $G_{F,Hyp}(s)$ is

$$P.I.[G_{F,Hyp}] \approx \frac{267.2}{84.6} \approx 3.2. \tag{4.3}$$

Using the IEEE Std 43-2013 [16] and by looking at the P.I. values alone, one could say that $G_{F,L3-L1}(s)$ failed the P.I. test while $G_{F,Hyp}(s)$ passed the test, since the minimum P.I. prescribed in Table 1 for a Class B insulation system is 2.0.

From this particular example, it is clear that there should be a certain parameter that would describe the dynamics in between the 1- and 10-minute insulation resistance measurements. It is therefore recommended to have a third measure which results in the proposed three-point polarization index (3PPI) definition below.

Definition. Let $IR_{10} > IR_\theta > IR_1$ be the insulation resistances measured in 10 mins., θ mins. and 1 min., respectively, where $10 > \theta > 1$. The *Three-Point Polarization Index (3PPI)* is defined as

$$3PPI \triangleq \gamma \frac{IR_{10} - IR_\theta}{IR_\theta - IR_1} + (1-\gamma)\frac{IR_{10}}{IR_1}, \tag{4.4}$$

for $0 < \gamma < 1$.

The proposed 3PPI is a function of two parameters: the usual P.I. on the second term of (4.4) which is defined in the IEEE Std 43-2013, and a certain ratio between three insulation resistance measures in the first term of (4.4). When $\gamma = 0$, then the 3PPI definition because the usual P.I. definition. However, when $\gamma = 1$, the 3PPI definition changes into a ratio of the between the difference of IR_{10} and IR_θ, and the difference of IR_θ and IR_1. The following research questions are then formed:

(1) What is the optimal value of θ for certain types of insulation systems?;
(2) What is the optimal value of γ?; and
(3) How low should $(IR_{10} - IR_\theta)/(IR_\theta - IR_1)$ be to say that the PMSM is in "good" condition?

A conjecture is then formed based on the definition of 3PPI:

Conjecture. A PMSM is "healthier" as $3PPI \to 0$.

5. **Conclusion and further research**

This paper has shown that a permanent magnet synchronous motor (PMSM) could have insulation resistance dynamics that is fractional-order in nature. As a consequence, the polarization index (P.I.) measure based on the IEEE Std 43-2013 definition may provide a misleading result if the dynamics of insulation resistance is not well-understood. The authors, therefore, recommend to measure a third insulation resistance value in between IR_1 and IR_{10} which is defined as IR_θ resulting in the proposed new "goodness" measure called Three-Point Polarization Index (3PPI) which is believe to be a better representation of how "good" or "healthy" a PMSM is.

To further advance this study, the authors recommend looking into how to find the optimal values of θ and γ which is assumed to be a function of the type of insulation resistance of the PMSM. To identify these optimal values, a series of exhaustive tests should be done by the research community using various test voltages and PMSMs.

Moreover, for further research would be better to use some exact method for instance maximum likelihood estimation method for estimating the model parameters θ and γ. We will use proposed technique for a class of the motors.

This paper has also shown the importance of the mathematics of fractional calculus and the application of fractional-order systems in the study of PMSM insulation resistance dynamics. A fractional-order system, in this context, is a generalization of the dynamical model of the PMSM in the assumption that we are constrained with the order at $0 < \alpha < 1$.

Acknowledgements

The authors would like to thank Engr. Michael John B. Castro, Engr. Rolly S. Presto and Engr. Michael Angelo D. Abalos of Jardine Schindler Elevator Corporation, 20/F Insular Life Corporate Center, Filinvest Alabang, Muntinlupa City, Philippines, and Marwan Radi of Jardine Schindler Group, 29/F Devon House, Taikoo Place, 979 King's Road, Quarry Bay, Hong Kong, for the series of discussions regarding the data obtained and presented in this paper. The authors also highly appreciate the guidance and help provided by Greg Stone of the P43 Working Group of the IEEE Std 43-2013 who has been instrumental in providing clarity about Polarization Index.

This work was supported in part by Portugese National Funds through the FCT–Foundation of Science and Technology under the Project PEst-UID/EEA/-00066/2013, the Slovak Grant Agency for Science under Grant VEGA 1/0908/15; the Slovak Research and Development Agency under the Contract: No. APVV-14-0892; Project ARO W911NF-15-1-0228 from USA; and COST Action CA15225 – a network supported by COST (European Cooperation in Science and Technology).

References

[1] G.L. Abulencia, A.C. Abad, Analog realization of a low-voltage two-order selectable fractional-order differentiator in a 0.35μm CMOS technology. In: *Internat. Conference on Humanoid, Nanotechnology, Information Technology, Communication and Control, Environment and Management*, Cebu City, Philippines, Dec. 9-12 (2015).

[2] R. Bartnikas, *Engineering Dielectrics, Vol. IIA, Electrical Properties of Solid Insulating Materials: Molecular Structure and Electrical Behavior.* American Society for Testing and Materials (ASTM), Philadelphia (1987).

[3] R. Bartnikas, *Engineering Dielectrics, Vol. IIB, Electrical Properties of Solid Insulating Materials: Measurement Techniques*, STP 926, American Society for Testing and Materials (ASTM), Philadelphia (1987).

[4] Y. Da, X. Shi, M. Krishnamurthy, A new approach to fault diagnostics for permanent magnet synchronous machines using electromagnetic signature analysis. *IEEE Trans. on Power Electronics* **28**, No 8 (2013).

[5] E. David, L. Lamarre, Progress in DC testing of generator stator windings: theoretical considerations and laboratory tests. *IEEE Transactions on Energy Conversion* **25**, No 1 (2010), 49–58.

[6] L. Dorčák, J. Valsa, E. Gonzalez, J. Terpák, I. Petráš, Analogue realization of fractional-order dynamical systems. *Entropy* **15**, No 10 (2013), 4199–4214.

[7] A. Erdelyi, *Higher Transcendental Functions*, Vol. 3. McGraw-Hill, New York (1955).

[8] M. Farhani, H. Borsi, E. Gockenback, M. Kaufhold, Partial discharge and dissipation factor behavior of model insulating systems for high voltage rotating machines under different stresses. *IEEE Electrical Insulation Magazine* **25**, No 5 (2005), 5–19.

[9] E.G. Gonzalez, Practical infrared thermography for lift system maintenance—a CBM approach to promote lift energy efficiency. In: *DLSU Research Congress 2014*, De La Salle University, Manila, Philippines, Mar. 6-8 (2014), SEE-I-006, 1–4.

[10] E.A. Gonzalez, M.J.B. Castro, R.S. Presto, M. Radi, I. Petráš, Fractional-order models in motor polarization index measurements. In: *17th IEEE Internat. Carpathian Control Conference (ICCC)*, High Tatras, Slovakia, May 29-Jun 1 (2016), 214–217.

[11] E.A. Gonzalez, L. Dorčák, C.B. Co, Bioelectrode models with fractional calculus. *Internat. J. of Intelligent Control and Systems* **17**, No 1 (2012), 7–13.

[12] E.A. Gonzalez, L. Dorčák, C.A. Monje, J. Valsa, F.S. Caluyo, I. Petráš, Conceptual design of a selectable fractional-order differentiator for industrial applications. *Fract. Calc. Appl. Anal.* **17**, No 3 (2014), 697–716; DOI: 10.2478/s13540-014-0195-z; https://www.degruyter.com/view/j/fca.2014.17.issue-3/issue-files/fca.2014.17.issue-3.xml.

[13] E.A. Gonzalez, I. Petráš, Advances in fractional calculus: control and signal processing applications. In: *16th IEEE Internat. Carpathian Control Conference*, Szilvasvarad, Hungary, 27-30 May (2015), 147–152.

[14] K.N. Gyftakis, M. Sumislawska, D.F. Kavanagh, D.A. Howey, M.D. McCulloch, Dielectric characteristics of electric vehicle traction motor

winding insulation under thermal aging. *IEEE Trans. on Industry Applications* **52**, No 2 (2016), 1398–1404.

[15] S.U. Haq, S.H. Jayaram, E.A. Cherney, G.G. Raju, Space charge analysis in enamelled wires by using thermally stimulated depolarization current (TDSC). *J. of Electrostatics* **67**, No 1 (2009), 12–17.

[16] *IEEE Recommended Practice for Testing Insulation Resistance of Electric Machinery*, IEEE Standard 43-2013, 2013.

[17] E. de Levie, On porous electrodes in electrolyte solutions: I. Capacitance effects. *Electrochimica Acta* **8**, No 10 (1963), 751–780.

[18] V. Martynyuk, M. Ortigueira, Fractional model of an electrochecmical capacitor. *Signal Processing* **107** (2015), 355–360.

[19] B. Milano, E. Eastment, B. Weeks, New insights and complications in determining generator stator insulation absorption current exponents and constants from polarization index test data. In: *IEEE Electr. Insulation Conference*, Montreal, Canada, May 31-Jun 3 (2009), 254–258.

[20] N.H. Obeid, T. Boileau, B. Nahid-Mobarakeh, Modeling and diagnostic of incipient inter-turn faults for a three-phase permanent magnet synchronous motor. *IEEE Trans. on Industry Applications* **52**, No 5 (2016), 4426–4434.

[21] P. Paloniemi, Multi-stress endurance tests on high-voltage motor insulations, with equal acceleration of each stress. *IEEE Trans. on Electrical Insulation* **EI-17**, No 3 (1982), 253–261.

[22] J. Petrzela, R. Sotner, M. Guzan, Implementation of constant phase elements using low-Q band-pass and band-reject filtering sections. In: *2016 IEEE Internat. Conference on Applied Electronics*, Pilsen, Czech Republic, 6-7 Sept. (2016), 205–210.

[23] I. Podlubny, *Fractional Differential Equations*. Academic Press, San Diego (1999).

[24] I. Podlubny, R. Magin, I. Trymorush, Niels Henrik Abel and the birth of fractional calculus. *Fract. Calc. Appl. Anal.* **20**, No 5 (2017), 1068–1075; DOI: 10.1515/fca-2017-0057; https://www.degruyter.com/view/j/fca.2017.20.issue-5/issue-files/fca.2017.20.issue-5.xml.

[25] G. Stone, Recent important changes in IEEE motor and generator winding insulation diagnostic testing standards. *IEEE Trans. on Industry Applications* **41**, No 1 (2005), 91–100.

[26] G.C. Stone, M. Sasic, Experience with DC polarization-depolarization measurements on stator winding insulation. In: *31st Electrical Insulation Conference (EIC)*, Ottawa, Canada (2013), 7–10.

[27] J.A. Tenreiro Machado, V. Kiryakova, The chronicles of fractional calculus. *Fract. Calc. Appl. Anal.* **20**, No 2 (2017), 307–336; DOI:

10.1515/fca-2017-0017; https://www.degruyter.com/view/j/fca.2017.20.issue-2/issue-files/fca.2017.20.issue-2.xml.

[28] H. Torkaman, F. Karimi, Measurement variations of insulation resistance/polarization index during utilizing time in HV electrical machines –A survey. *Measurement* **59** (2015), 21–29.

[29] J. Valsa, P. Dvořák, M. Friedl, Network model of the CPE. *Radioengineering* **20**, No 3 (2011), 619–626.

[30] K.J. Vetter, *Electrochemical Kinetics*. Academic Press, New York (1967).

[31] J.C. Wang, Realizations of generalized Warburg impedance with RC ladder networks and transmission lines. *J. of Electrochemical Soc.* **134**, No 8 (1987), 1915–1920.

[32] E. Warburg, Ueber die polarisationscapacität des platins. *Annalen der Physic* **331**, No 9 (1901), 125–135.

[33] Z. Zhang, H.-B. Li, Z.-H. Li, A novelty digital algorithm for online measurement of dielectric loss factor for electronic transformers. *Measurement* **43**, No 3 (2013), 1200–1207.

[1] *Schindler Elevator Corporation*
1530 Timberwolf Dr, Ste. B, Holland, OH
43528-9161, USA

e-mail: emmgon@gmail.com

[2] *Technical University of Košice*
Faculty of BERG, B. Němcovej 3
042 00 Košice, SLOVAK Republic

e-mail: ivo.petras@tuke.sk

Received: February 20, 2017

[3] *UNINOVA and DEE/ Faculdade de Ciências e Tecnologia da UNL*
Campus da FCT, Quinta da Torre
2829-516 Caparica, PORTUGAL

e-mail: mdo@fct.unl.pt

Please cite to this paper as published in:

Fract. Calc. Appl. Anal., Vol. **21**, No 3 (2018), pp. 613–627,
DOI: 10.1515/fca-2018-0033